Chemical Engineering Journal 148 (2009) 480–487

Contents lists available at ScienceDirect

Chemical Engineering Journal

journal homepage: www.elsevier.com/locate/cej

Adsorption kinetics and equilibrium of copper from aqueous solutions using hazelnut shell activated carbon

E. Demirbas[a,*], N. Dizge[b], M.T. Sulak[b], M. Kobya[b]

[a] Gebze Institute of Technology, Department of Chemistry, 41400, Gebze, Turkey
[b] Gebze Institute of Technology, Department of Environmental Engineering, 41400, Gebze, Turkey

ARTICLE INFO

Article history:
Received 6 March 2008
Received in revised form
15 September 2008
Accepted 20 September 2008

Keywords:
Hazelnut shell carbon
Desorption
Copper ions
Adsorption kinetics
Adsorption equilibrium

ABSTRACT

The adsorption of Cu(II) ions from aqueous solutions by hazelnut shell activated carbon (HSAC) was studied in a batch adsorption system. Factors influencing copper adsorption such as initial copper ion concentration (25–200 mg L^{-1}), pH (2–6), adsorbent dosage (0.5–3.0 g L^{-1}) and temperature (293–323 K) were investigated. The adsorption process was relatively fast and equilibrium was established about 90 min. Maximum adsorption of Cu(II) ions occurred at around pH 6. A comparison of the kinetic models on the overall adsorption rate showed that the adsorption system was best described by the pseudo second-order kinetics. Desorption experiments were carried out to test the performance of the carbon and desorption efficiencies in four cycles were found to be in the range 74–79%. The adsorption equilibrium data fitted best with the Langmuir isotherm and the monolayer adsorption capacity of Cu(II) ions was determined as 58.27 mg g^{-1} at 323 K. Thermodynamic parameters were calculated for the Cu(II) ion–HSAC system and the positive value of ΔH (18.77 kJ mol^{-1}) showed that the adsorption was endothermic and physical in nature.

1. Introduction

Copper is heavily used metal in industries such as plating, mining and smelting, brass manufacture, electroplating industries, petroleum refining and excessive use of Cu-based agrichemicals mining. These industries produce much wastewater and sludge containing Cu(II) ions with various concentrations, which have negative effects on the water environment [1]. Copper may be also found as a contaminant in food, especially shellfish, liver, mushrooms and nuts [2]. It has been reported that excessive intake of copper by humans may lead to severe mucosal irritation, hepatic and renal damage, widespread capillary damage, capillary damage, and central nervous problems [3]. The World Health Organization recommended a maximum acceptable concentration of Cu(II) in drinking water of 1.5 mg L^{-1} [4]. Therefore, the concentration of this metal must be reduced to level that satisfy environmental regulations for various bodies of water.

The most commonly used techniques for removing of Cu(II) ion from aqueous solutions include oxidation, reduction, precipitation, membrane filtration, biological process, ion exchange and adsorption. Among various treatment technologies, activated carbon adsorption is commonly used due to its porous surface structure, which provides it with a high surface area, harmlessness to the environment and ease in operation. However, the high cost of activated carbon has led to the development of new adsorbents with similar characteristics, but lower costs [5,6]. Therefore, there is a need to search into alternatives to investigate low-cost, effective and economical adsorbents. Several research workers have studied the production of activated carbon from *Ceiba pentandra* hulls carbon [4], pecan shell carbon [7,8], hazelnut shell carbon [9–12], peanut hull carbon [13], coirpith carbon [14,15], olive stones and walnut shells [16], almond shell carbon [17,18], peach stone carbon [17,19], olive stone carbon [17,20] and sawdust carbon [21].

In this study, waste hazelnut shell was utilized as the raw material for the production of granular activated carbon by chemical activation and its adsorption capacity for Cu(II) ions from aqueous solutions was evaluated. Effects of initial metal ion concentration, pH, adsorbent dosage and temperature on hazelnut shell activated carbon (HSAC) under kinetic and equilibrium conditions were investigated. Thermodynamic parameters were also calculated.

2. Experimental

2.1. Materials and characterizations

Hazelnut shell is an important agricultural residue and the amount produced annually in Turkey is estimated to be about 3×10^5 tons [22]. At present, this agricultural waste material is

* Corresponding author. Tel.: +90 262 6053108; fax: +90 262 6053101.
E-mail address: erhan@gyte.edu.tr (E. Demirbas).

1385-8947/$ – see front matter © 2008 Elsevier B.V. All rights reserved.
doi:10.1016/j.cej.2008.09.027

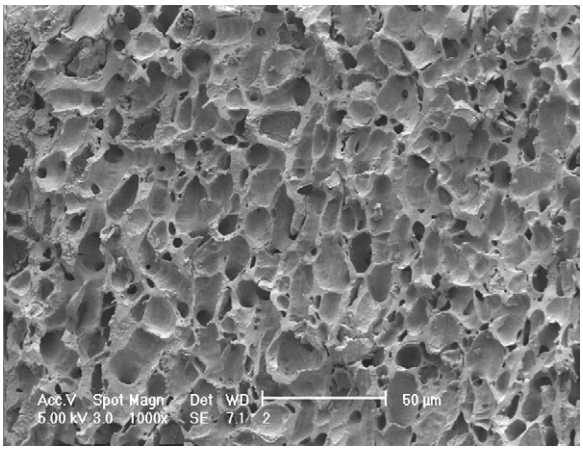

Fig. 1. Typical SEM micrograph of HSAC particle (magnification: 1000×).

used principally as a solid fuel. Carbon for HSAC was obtained from species of *Corylus avellana* from Trabzon in Turkey. Analytical grade reagents were used in all the experiments and water was purified by means of a Milli-Q system (Millipore). Carbon was air-dried and crushed with geometrical mean size ranging from 1.0 to 1.2 mm. 100 g of the selected fraction was impregnated with concentrated H_2SO_4. Then it was activated in a hot air oven at 200 °C for 24 h. The carbonized material was washed with distilled water to remove the free acid and the carbon was soaked in 1% $NaHCO_3$ solution to remove any remaining acid. Then it was washed with distilled water until the pH of the activated carbon reached 6, dried at 105 °C. The surface area of HSAC was measured by BET (Brunauer–Emmett–Teller nitrogen adsorption technique). The bulk density of the adsorbent was determined with a densitometer. The bulk density, ash content, moisture, solubility in water, solubility in acid, surface area and iodine number of HSAC were determined as 0.54 g cm^{-3}, 2.04%, 7.84%, 0.82%, 1.14%, 441 m^2 g^{-1} and 204 mg g^{-1}, respectively. The surface of adsorbent was characterized by scanning electron microscopy (SEM, Philips XL30S-FEG). HSAC had considerable numbers of pores where the metal ion was trapped and adsorbed into these pores (Fig. 1). The FTIR spectroscopy method was used to get information on interactions between the functional groups of the carbon and the copper ion. The infrared spectra of the samples were recorded in the range 4000–400 cm^{-1} on a BioRad FTS 175C spectrophotometer using a pellet technique (figure not shown). The samples were prepared mixing 1 mg of material with 100 mg of spectroscopy grade KBr. The adsorption bands at 3631, 3055, 1707, 1618 and 896 cm^{-1} were assigned to –OH, –C–H, –C=O, –C=C, and –C=CH_2, respectively which indicated the complex nature of the adsorbent. The main functional groups involved in the binding of copper ions suggested that the mechanisms of copper adsorption on HSAC could occur by surface complexation.

2.2. Batch mode adsorption studies

The effects of experimental parameters such as, initial metal ion concentration (25–200 mg L^{-1}), pH (2–6), adsorbent dosage (0.5–3.0 g L^{-1}) and temperature (293–323 K) on the adsorptive removal of Cu(II) ions were studied in a batch mode of operation for a specific period of contact time (0–120 min). The Cu(II) solutions were prepared by dissolving $CuSO_4{\cdot}5H_2O$ in distilled water and used as a stock solution and diluted to the required initial concentration. pH was adjusted using 0.1N HCl or 0.1N NaOH. For kinetic studies, 50 mL of Cu(II) solution of known initial concentration and initial pH was taken in a 250 mL screw-cap conical flask with a fixed adsorbent dosage (3 g L^{-1}) and was agitated in a thermostated rotary shaker for a contact time varied in the range 0–120 min at a speed of 300 rpm at 293 K. At various time intervals, the adsorbent was separated from the samples by filtering and the filtrate was analysed using a PerkinElmer model SIMAA 6000 atomic absorption spectrometer at a wavelength of 324.8 nm. Quality assurance of analytical measurements was performed in this study. Copper atomic spectroscopy standard solution of 1000 mg L^{-1} ± 0.3% (Merck) was used for measurements. Calibration curves between 1 and 20 mg L^{-1} were prepared and detection limit was found as 1 mg L^{-1}. Precision of the parallel measurements was as ±3% SD. For adsorption isotherms, different initial Cu(II) ion concentrations (50–1000 mg L^{-1}) were agitated with 3 g L^{-1} adsorbent dosage in a thermostated shaker at 300 rpm for 240 min. The adsorbent was separated and the metal under consideration was determined as mentioned previously. The concentration retained in the adsorbent phase (q_e, mg g^{-1}) was calculated by using the following equation

$$q_e = \frac{(C_o - C_t)V}{W} \quad (1)$$

where C_o is the initial Cu(II) concentration and C_t is the Cu(II) concentration (mg L^{-1}) at any time, V is the volume of solution (L) and W is the mass of the adsorbent (g). The data analysis was carried out using correlation analysis employing least-square method and the sums of error squares (SSE) is calculated using the following equation

$$\mathrm{SSE} = \sqrt{\frac{\sum (q_{e,\exp} - q_{e,\mathrm{calc}})^2}{N}} \quad (2)$$

where N is the number of data points. Each experiment was conducted in triplicate under identical conditions to confirm the results, and was found reproducible (experimental error within 3%).

3. Adsorption kinetics

Kinetic study is important to an adsorption process because it depicts the uptake rate of adsorbate, and controls the residual time of the whole adsorption process. Four kinetic models, pseudo first-order [23], pseudo second-order [24], Elovich [25] and diffusion kinetic models [26], are selected in this study for describing the adsorption process.

3.1. The pseudo first-order equation

A pseudo first-order equation can be expressed in a linear form as

$$\log(q_e - q_t) = \log(q_e) - \frac{k_1}{2.303}(t) \quad (3)$$

where q_e and q_t are the amount of copper ions adsorbed (mg g^{-1}) on the adsorbent at the equilibrium and at time t, respectively, and k_1 is the rate constant of adsorption (L min^{-1}). Values of k_1 were calculated from the plots of $log(q_e - q_t)$ versus t for different concentrations of the Cu(II) ion. The values k_1 and q_e are given in Table 1.

3.2. The pseudo second-order equation

A linear form of pseudo second-order model is shown in Eq. (4)

$$\frac{t}{q_t} = \frac{1}{k_2 q_e^2} + \frac{1}{q_e}(t) \quad (4)$$

where k_2 is the rate constant of pseudo second-order adsorption (g mg^{-1} min^{-1}). The constants can be obtained from plotting (t/q_t) versus t. The values k_2, q_e and h ($k_2 q_e^2$) are given in Table 1.

Table 1
The pseudo first-order and second-order kinetic parameters for Cu(II) at different pHs, initial dye concentrations and adsorbent dosages by HSAC.

Parameters	Pseudo first-order kinetic					Pseudo second-order kinetic				
	$q_{e,exp}$ (mg g^{-1})	$q_{e,calc}$ (mg g^{-1})	k_1 (L min^{-1})	r^2	SSE (%)	$q_{e,calc}$ (mg g^{-1})	k_2 (g mg^{-1} min^{-1})	$h = k_2 q_e^2$ (mg g^{-1} min^{-1})	r^2	SSE (%)
pH										
2.0	9.02	8.77	0.0359	0.998	3.54	10.91	0.0179	2.128	0.994	1.91
3.0	14.67	14.68	0.0447	0.993	1.12	18.68	0.0041	1.439	0.993	4.01
4.0	15.04	14.11	0.0432	0.998	3.13	17.75	0.0034	1.066	0.997	2.75
5.0	15.02	14.19	0.0496	0.999	8.58	16.94	0.0027	0.948	0.998	2.39
6.0	15.33	14.38	0.0428	0.999	5.75	16.00	0.0018	0.493	0.998	1.11
C_o (mg L^{-1})										
25	8.06	8.16	0.1050	0.996	0.93	8.77	0.0121	0.964	0.996	0.77
50	15.33	14.38	0.0428	0.999	5.75	16.00	0.0018	0.493	0.998	1.11
100	29.33	20.50	0.0381	0.991	80.14	30.52	0.0002	0.219	0.998	1.19
200	36.33	25.48	0.0598	0.988	61.44	37.76	0.00008	0.117	0.999	1.43
m_s (g L^{-1})										
0.5	58.00	25.10	0.0346	0.965	263.40	50.66	0.00003	0.076	0.999	0.66
1.5	41.26	21.48	0.0337	0.972	231.03	41.74	0.00006	0.108	0.998	0.74
2.0	23.18	12.16	0.0391	0.944	100.76	23.61	0.00031	0.176	0.998	0.61
3.0	15.33	14.38	0.0428	0.999	5.75	16.00	0.0018	0.493	0.998	1.11

3.3. The Elovich equation

The Elovich model equation [25] is generally expressed as:

$$\frac{dq_t}{dt} = \alpha \exp(-\beta q_t) \quad (5)$$

where α is the initial adsorption rate (mg g^{-1} min^{-1}) and β is the desorption constant (g mg^{-1}) during any one experiment. To simplify the Elovich equation, $\alpha\beta t \gg t$ is assumed and by applying the boundary conditions $q_t = 0$ at $t = 0$ and $q_t = q_t$ at $t = t$ equation becomes:

$$q_t = \frac{1}{\beta}\ln(\alpha\beta) + \frac{1}{\beta}\ln(t) \quad (6)$$

A plot of q_t versus $\ln(t)$ should yield a linear relationship with a slope of $(1/\beta)$ and an intercept of $(1/\beta)\ln(\alpha\beta)$. The constants are listed in Table 2.

3.4. Diffusion kinetic model

Diffusion kinetic model [26], D, is the sum of pore and surface diffusion. It may be calculated from the following equation

$$-\log\left(1 - \left(\frac{q_t}{q_e}\right)^2\right) = \left(\frac{4\pi^2 D}{2.3d^2}\right)t \quad (7)$$

where d is the mean particle diameter (cm), respectively. By plotting $-\log(1-(q_t/q_e)^2)$ against t, D (cm^2 s^{-1}) may be determined from the kinetic adsorption data. Values of D are given in Table 2.

4. Results and discussion

4.1. Adsorption kinetics

4.1.1. Effect of initial Cu(II) concentration on adsorption kinetics

The adsorption capacity of Cu(II) increased with time and attained a maximum value at 60 min and thereafter, it reached a constant value indicating that no more Cu(II) ions were further removed from the solution (Fig. 2). The equilibration time was found to be around 90 min but the adsorption experiments for practical reasons were run for 120 min. On changing the initial concentration of Cu(II) solution from 25 to 200 mg L^{-1}, the amount adsorbed increased from 8.0 to 36.3 mg g^{-1} (Fig. 2). This may be attributed to an increase in the driving force of the concentration gradient with the increase in the initial copper concentration in order to overcome all mass transfer resistance of Cu(II) ions between the aqueous and solid phases. Therefore, a higher initial concentration of Cu(II) ions may increase the adsorption capacity [27].

The experimental data for the adsorption of the copper ion onto HSAC treated with the above kinetic models were used to evaluate the controlling mechanism of adsorption processes. The higher correlation coefficients (r^2) values and lowest SSE values confirmed that the adsorption data were well represented by pseudo second-order kinetics for the entire adsorption period (Table 1). Values from the calculated equilibrium adsorption capacities ($q_{e,calc}$) agreed well with the experimental data ($q_{e,exp}$) for the second-order kinetic model as well (Table 1).

The values of the second order rate constants (k_2) were found to decrease from 1.21×10^{-2} to 8×10^{-5} g mg^{-1} min^{-1} as the initial concentration increased from 25 to 200 mg L^{-1}, showing the process to be highly concentration dependent, which is consistent with studies reported [28]. The values of the initial adsorption rates, h determined from the straight line plots for each adsorbent system, increased with decrease in the initial copper concentration as given in Table 1. The lower the concentration of copper ions in the

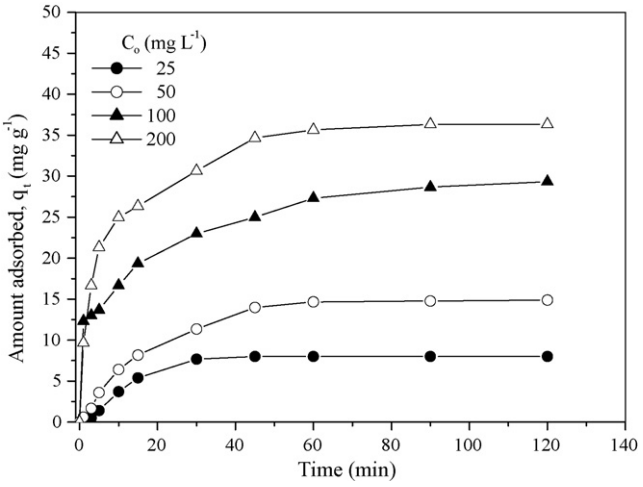

Fig. 2. Effect of initial concentration on the adsorption of Cu(II) by HSAC (*Conditions*: pH 6, 1.00–1.20 mm particle size, 3 g L^{-1} adsorbent dosage, 300 rpm, 120 min agitation time and 293 K).

Table 2
The Elovich and intraparticle diffusion kinetic parameters for Cu(II) at different pHs, initial dye concentrations and adsorbent dosages by HSAC.

Parameters	Elovich kinetic model						Diffusion kinetic model			
	$q_{e,exp}$ (mg g^{-1})	$q_{e,calc}$ (mg g^{-1})	α (mg g^{-1} min^{-1})	β (g mg^{-1})	r^2	SSE (%)	$q_{e,calc}$ (mg g^{-1})	$D \times 10^{-5}$ (cm^2 s^{-1})	r^2	SSE (%)
pH										
2.0	9.02	8.89	1.41	0.499	0.971	5.02	16.7	1.284	0.986	7.69
3.0	14.67	15.08	2.23	0.288	0.975	8.21	23.7	1.765	0.988	9.03
4.0	15.04	15.53	2.66	0.292	0.980	8.01	24.5	1.832	0.997	9.50
5.0	15.02	15.67	3.42	0.309	0.981	7.44	23.5	1.777	0.991	8.49
6.0	15.33	15.75	6.05	0.294	0.981	8.04	24.9	2.496	0.996	6.71
C_o (mg L^{-1})										
25	8.06	9.09	2.69	0.575	0.967	4.21	10.2	1.628	0.986	2.19
50	15.33	15.75	6.05	0.294	0.981	8.04	24.9	2.496	0.996	6.71
100	29.33	29.30	26.35	0.224	0.989	11.01	49.9	2.596	0.996	20.57
200	36.33	38.21	49.60	0.183	0.992	12.00	51.3	4.156	0.991	14.97
m_s (g L^{-1})										
0.5	58.00	49.31	836.25	0.201	0.988	12.85	93.1	1.518	0.984	43.10
1.5	41.26	39.62	743.77	0.253	0.956	10.85	72.7	1.470	0.990	31.72
2.0	23.18	22.82	319.75	0.425	0.975	5.94	73.5	1.655	0.969	50.50
3.0	15.33	15.75	6.05	0.294	0.981	8.04	24.9	2.496	0.996	6.71

solution, the lower the probability of collisions among Cu(II) ions, therefore Cu(II) ions could be bonded to the active sites in a shorter period of time [29]. For the present systems, the values of the diffusion coefficient shown in Table 2 fall well within the magnitudes reported in literature [30], specifically for chemisorption systems (10^{-5} to 10^{-13} cm^2 s^{-1}). The corresponding diffusion coefficients for the various concentrations of Cu(II) ions varied from 1.63×10^{-5} to 4.16×10^{-5} cm^2 s^{-1}. The increase in D values was attributed to the increase in the internal surface affinity [31].

4.1.2. Effect of pH on adsorption kinetics

The pH of an aqueous solution is an important controlling parameter in the process of adsorption. Experiments were carried out in the pH range 2–6 since copper started to precipitate as $Cu(OH)_2$ above pH 6. This has been confirmed by the speciation diagram shown in Fig. 3 [32]. The dominant species of copper is free Cu^{2+} below pH 6 and mainly involved in adsorption process. The amounts of copper adsorbed increased gradually from 9.0 to 15.3 mg g^{-1} as pH increased from 2 to 6 (figure not shown). At very low pH values, copper adsorption was found to be very low due to competition between H_3O^+ and Cu(II) ions for the adsorption sites. The original pH of copper solution was 6 and the subsequent experiments were carried out at this pH.

The effect of pH can be also explained by considering the surface charge on the adsorbent material. The zero charge of the adsorbent (pH_{pzc}, Zetameter 3) was determined as 5.8 which is the point at which the net charge of the adsorbent is zero (Fig. 4). The pH of solution was 6 and was higher than pH_{pzc}. Thus, the activated carbon adsorbent acts as a negative surface and attracts the positively charged metal ions. Generally, the net positive charge decreases with increasing pH value and leads to decrease in the repulsion between the adsorbent surface and metal ions and thus, enhances the adsorption capacity [33].

The experimental data showed good compliance with the pseudo second-order kinetic model in terms of higher correlation coefficients ($r^2 > 0.99$) and very close values between $q_{e,calc}$ and $q_{e,exp}$. Values of D for the Cu(II) adsorption on HSAC varied from 1.28×10^{-5} to 2.50×10^{-5} cm^2 s^{-1} as pH was increased from 2 to 6 (Table 2). This indicated that the transport of Cu(II) ions from solution through the particle solution interface into the pores of the particles as well as the adsorption on the available surface of adsorbents are both responsible for the uptake of Cu(II) ions.

4.1.3. Effect of adsorption dosage on adsorption kinetics

Adsorbent dosage is an important parameter because it determines the capacity of an adsorbent for a given initial concentration of the adsorbate. The effect of adsorbent dosage was studied on Cu(II) ion removal from aqueous solutions by varying the amount of HSAC from 0.5 to 3.0 g L^{-1}, while keeping other parameters (pH, agitation speed, temperature and contact time) constant. Fig. 5 showed that the amount of Cu(II) ion adsorbed increased from 15.0 to 58.0 mg g^{-1} for HSAC as the adsorption dosage was decreased from 3 to 0.5 g L^{-1}. On the other hand, the amount adsorbed per unit mass of the adsorbent decreased considerably. The decrease in unit adsorption with increase in the dosage of adsorbent was due

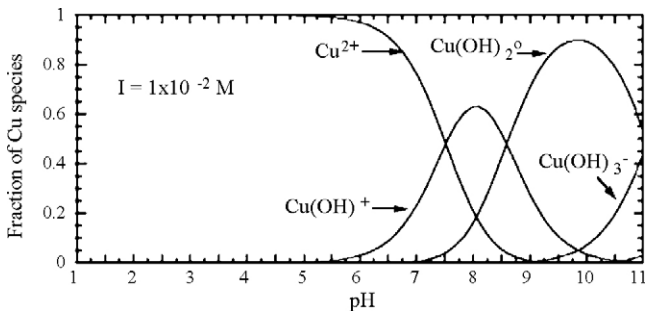

Fig. 3. Distribution of Cu(II) species as a function of pH.

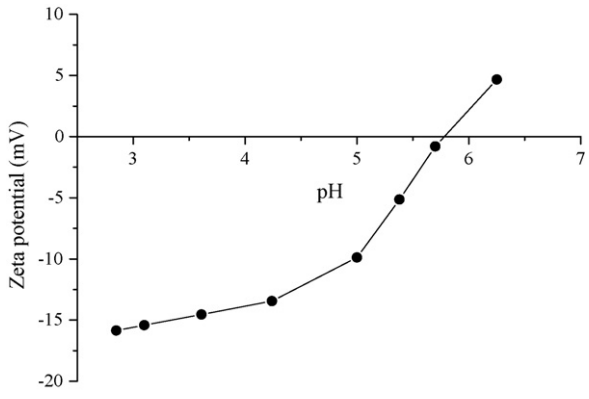

Fig. 4. The zeta potential curves as a function of pH for HSAC.

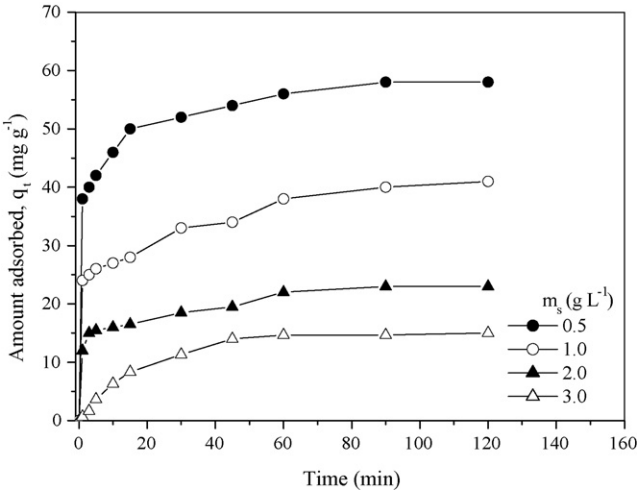

Fig. 5. Effect of adsorbent dosage on the adsorption of Cu(II) by HSAC (*Conditions*: 50 mg L^{-1}, pH 6, 1.00–1.20 mm particle size, 300 rpm, 120 min agitation time and 293 K).

to adsorption sites remaining unsaturated during the adsorption process [34]. For the rest of the study 3 g L^{-1} adsorbent dosage is considered as optimum dosage for copper removal using HSAC.

The kinetic parameters calculated from the kinetic models are shown in Table 1. The experimental data fit well with the pseudo second-order kinetic model ($r^2 > 0.99$). Values of k_2 increased from 3.0×10^{-5} to 1.80×10^{-3} (g mg^{-1} min^{-1}) with the increase in adsorbent dosage which resulted in an increase in the surface area for adsorption and an increase in the available sites for adsorption.

4.2. Adsorption isotherms

Equilibrium relationships between adsorbent and adsorbate are described by adsorption isotherms. Three adsorption isotherm equations (8)–(10) were used in the present study namely, Langmuir [35], Freundlich [36] and Tempkin [37]. The applicability of the isotherm models to the adsorption study done was compared by judging the correlation coefficients values. The linear forms of the Langmuir, Freundlich and Tempkin isotherms are represented by the following equations:

$$\frac{C_e}{q_e} = \frac{1}{Q_0 b} + \frac{C_e}{Q_0} \tag{8}$$

where C_e is the equilibrium concentration (mg L^{-1}), Q_o is the monolayer adsorption capacity (mg g^{-1}) and b is the constant related to the free adsorption energy (Langmuir constant, L mg^{-1}).

$$\log q_e = \log k_F + \frac{1}{n} \log C_e \tag{9}$$

where k_F is a constant indicative of the adsorption capacity of the adsorbent (mg g^{-1}) and the constant $1/n$ indicates the intensity of the adsorption.

$$q_e = \left(\frac{RT}{b_T}\right) \ln A + \left(\frac{RT}{b_T}\right) \ln C_e \tag{10}$$

where A (L g^{-1}) and b_T (J mol^{-1}) are the Tempkin constants. The theoretical parameters of adsorption isotherms along with regression coefficients are listed in Table 3. The Langmuir isotherm model had highest values of regression coefficients when compared to the rest of isotherm models, which showed the homogeneous nature of the adsorbent. The maximum adsorption capacity and Langmuir constant were calculated from the slope and intercept of the linear plots C_e/q_e versus C_e which gives a straight line of slope $1/Q_o$ which corresponds to complete monolayer coverage (mg g^{-1}) and the intercept is $1/Q_o b$. The maximum capacity for monolayer saturation was 58.27 mg Cu(II) per gram of the adsorbent material at 323 K because high temperatures led to a higher chance of the copper ion being adsorbed onto the adsorbent and an increase in its adsorption capacity which results in the enlargement of pore size.

4.2.1. Effect of temperature

Adsorption experiments were conducted at 293, 303, 313 and 323 K to investigate the effect of temperature, with initial Cu(II) concentration of 50–1000 mg L^{-1}, adsorbent dosage of 3 g L^{-1}, pH 6 and particle size of 1.00–1.20 mm. It was observed that the maximum adsorption capacity of Cu(II) ion increased from 48.6 mg g^{-1} at 293 K to 58.3 mg g^{-1} at 323 K, i.e. adsorption increased with the increase of temperature (figure not shown). This can be explained by the fact that at higher temperature, the kinetic energy of Cu^{2+} cations is high; therefore, contact between Cu^{2+} and the active sites of HSAC is sufficient, leading to an increase in adsorption efficiency. This condition shows that adsorption is more of a physical than a chemical adsorption. Similar trends are also observed by other researchers for aqueous phase adsorption [38]. In addition to that, the rise of adsorption with temperature may enlarge the pore size to some extent which may also affect the carbon adsorption capacity.

Thermodynamic parameters such as change in free energy (ΔG°), enthalpy (ΔH°) and entropy (ΔS°) were calculated using the following equations:

$$\Delta G^\circ = -2.303\, RT \log K \tag{11}$$

$$\log K = \frac{\Delta S^\circ}{2.303R} - \frac{\Delta H^\circ}{2.303R}\left(\frac{1}{T}\right) \tag{12}$$

Table 4
Thermodynamic parameters for the adsorption of Cu(II) in aqueous solutions onto HSAC.

T (K)	Thermodynamic parameters		
	ΔG (kJ mol^{-1})	ΔH (kJ mol^{-1})	ΔS (J mol^{-1} K^{-1})
293	6.83		
303	6.66	18.77	40.4
313	6.03		
323	5.71		

Table 3
Langmuir, Freundlich and Tempkin isotherm parameters and correlation coefficients for the adsorption of Cu(II) in aqueous solutions onto HSAC at different temperatures.

T (K)	Langmuir isotherm			Freundlich isotherm			Tempkin isotherm		
	Q_o (mg g^{-1})	b (L mg^{-1})	r^2	k_f (mg g^{-1})	n	r^2	b_T (J mol^{-1})	A (L mg^{-1})	r^2
293	48.64	0.0054	0.999	10.183	3.907	0.915	379.97	3.419	0.975
303	51.52	0.0053	0.999	11.458	4.087	0.943	397.53	5.198	0.989
313	55.40	0.0033	0.999	16.962	5.255	0.959	406.79	9.396	0.990
323	58.27	0.0252	0.999	19.208	5.563	0.967	429.38	18.580	0.992

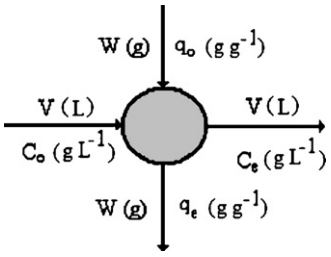

Fig. 6. A single-stage batch adsorber.

where K (=b) is the adsorption isotherm constant, R is the gas constant (8.314 J K^{-1} mol^{-1}), T is the absolute temperature, respectively. ΔH° and ΔS° can be calculated from the slope and intercept of the Van't Hoff plot of log K versus (1/T) from Eq. (12). Positive value of ΔH° indicates that the adsorption process is endothermic. ΔG° reflects the feasibility of the process and standard entropy determines the disorderliness of the adsorption at solid–liquid interface (Table 4).

4.2.2. Single-stage batch adsorber

Adsorption isotherm studies can also be used to predict the design of single stage batch adsorption systems [39,40]. The schematic diagram for a single-stage adsorption process is shown in Fig. 6. The solution to be treated contains V L of solvent and the pollutant concentration is reduced from C_o to C_e in the adsorption process. The amount of adsorbent added is W g of adsorbate-free solid and the metal concentration changes from $q_o = 0$ to q_e. The mass balance equates the metal removed from the liquid to that picked up by the adsorbent is

$$V(C_o - C_e) = W(q_e - q_o) = Wq_e \quad (13)$$

The Langmuir isotherm data may now be applied to Eq. (13) since the Langmuir isotherm gave the best fit to experimental data.

$$\frac{W}{V} = \frac{C_o - C_e}{q_e} = \frac{C_o - C_e}{[(Q_o bC_e)/(1 + bC_e)]} \quad (14)$$

Fig. 7 shows a series of plots derived from Eq. (14) for the adsorption of Cu(II) ions on the adsorbent and depicts the amount of effluent which can be treated to reduce the copper content by 90, 80, 70, 60 and 50% using various masses of the adsorbent.

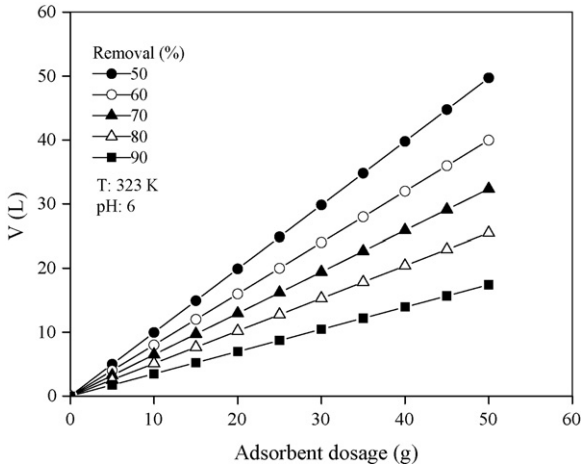

Fig. 7. Volume of effluent (V) treated against adsorbent mass (W) for different percentage copper removal.

Table 5
Adsorption capacity of Cu(II) by various adsorbents.

Adsorbent	Q_o (mg g^{-1})	Reference
Pecan shell carbon	95.00	[7]
Peanut hull carbon	65.57	[13]
HSAC	58.27	This study
Hazelnut shell carbon	39.54	[12]
NaOCl-modified CNTs	47.39	[41]
Coirpith carbon	39.70	[14]
Ceiba pentandra hulls carbon	20.80	[4]
Olive stone carbon	9.21	[17]
Almond shell carbon	8.85	[17]
Peach stone carbon	7.21	[17]
Sawdust carbon	5.73	[21]

4.2.3. Comparison of HSAC with other adsorbents

Several studies have been conducted using various types of adsorbents for Cu(II) adsorption. Table 5 presents a comparison of the adsorption capacity of the results. It can be seen from the table that HSAC shows the comparable adsorption capacity with respect to other adsorbents, revealing that HSAC is suitable for the removal of Cu(II) from aqueous solutions since it has a relatively high adsorption capacity.

4.2.4. Desorption studies

Desorption experiments were carried out in order to estimate the metal releasing capacity of HSAC loaded with Cu(II) ions. Each adsorption (HSAC–25 mg L^{-1} of Cu(II)) and desorption cycle (Cu(II) loaded HSAC–1.0N HCl) was allowed 120 min of contact time at 293 K and consecutive adsorption–desorption cycles were repeated four times using the same adsorbent in solutions (Fig. 8). The adsorption and desorption efficiencies of the carbon from the four cycles were 96, 95, 93, 92% for adsorption and 79.2, 78.3, 75.0, 73.9% for desorption, respectively. There was a slight decrease in both the percentage of Cu(II) ion adsorbed and the percentage of Cu(II) ion desorbed from the first to the fourth cycle. This showed that the carbon was restored close to the original condition without damage to the nature of the adsorption characteristics of the carbon.

Similarly, desorption kinetics was also studied separately with 0.1, 0.5 and 1.0 N HCl for 25, 100 and 200 mg L^{-1} of Cu(II) solutions. Liquid samples were withdrawn at predetermined time intervals and the sample was filtrated. The residual copper ion concentration in solution was analyzed with atomic adsorption spectrophotometry. The kinetic results were presented in Table 6. The higher r^2

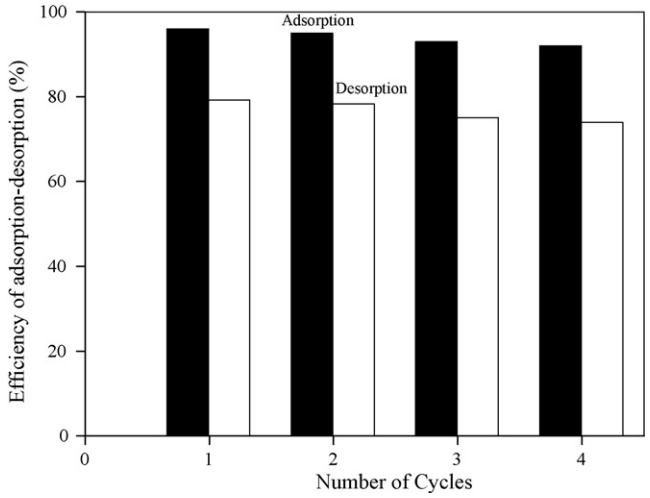

Fig. 8. The performance of HSAC by multiple cycles of regeneration.

Table 6
The desorption kinetic parameters for Cu(II) loaded HSAC at different HCl concentrations for various Cu(II) solutions.

C_o (mg L^{-1})	HCl (N)	Pseudo first-order kinetic				Pseudo second-order kinetic			
		$q_{e,exp}$ (mg g^{-1})	$q_{e,calc}$ (mg g^{-1})	k_1 (L min^{-1})	r^2	$q_{e,calc}$ (mg g^{-1})	k_2 (g g^{-1} min^{-1})	$h = k_2 q_e^2$ (mg g^{-1} min^{-1})	r^2
25	0.1	5.33	3.91	0.0412	0.995	5.69	0.0216	0.700	0.998
	0.5	5.67	3.59	0.0446	0.944	5.96	0.0298	1.058	0.999
	1.0	6.00	3.33	0.0405	0.958	6.22	0.0329	1.274	0.999
50	0.1	7.67	3.77	0.0580	0.957	7.88	0.0443	2.752	0.999
	0.5	9.00	4.10	0.0392	0.950	9.21	0.0302	2.864	0.999
	1.0	9.33	3.32	0.0389	0.951	9.48	0.0423	3.802	0.999
200	0.1	18.02	15.57	0.0786	0.991	19.23	0.0088	3.259	0.998
	0.5	22.01	14.23	0.0708	0.969	22.88	0.0119	6.211	0.999
	1.0	24.01	15.64	0.0737	0.971	24.95	0.0111	6.896	0.999

values and close values between $q_{e,calc}$ and $q_{e,exp}$ confirmed that the desorption data were well represented by pseudo second-order kinetics (Table 6).

5. Conclusion

The adsorption of copper on the activated carbon is found to be initial metal ion concentration, solution pH, time, adsorbent dosage and temperature dependent. Adsorption process revealed that the initial uptake was rapid and equilibrium was achieved in about 90 min. The optimum parameters for this study were pH 6, 50 mg L^{-1} of Cu(II) concentration and 3 g L^{-1} of adsorbent dosage. Experimental results indicated that the pseudo second-order reaction kinetics provided the best description of the data. Desorption studies were carried out using various concentrations of hydrochloric acid solution. The adsorption–desorption cycles showed that the adsorbent could be used for a minimum four cycles. The isotherm study indicated that adsorption data correlated well with Langmuir isotherm model. Thermodynamical parameters were also evaluated for the metal ion–adsorbent system and revealed that the adsorption was endothermic in nature. This study demonstrated that the HSAC could be used as an effective adsorbent for the treatment of wastewater containing Cu(II) ions.

References

[1] N. Li, N. Bai, Copper adsorption on chitosan-cellulose hydrogel beads: behaviours and mechanisms, Sep. Purif. Technol. 42 (2005) 237–247.
[2] W.M. Antunes, A.S. Luna, C.A. Henriques, A.C.A. Costa, An evaluation of copper biosorption by a brown seaweed under optimised conditions, Electron. J. Biotechnol. 6 (2003) 174–184.
[3] S. Larous, A.H. Meniai, M.B. Lehocine, Experimental study of the removal of copper from aqueous solutions by adsorption using sawdust, Desalination 185 (2005) 483–490.
[4] M.M. Rao, A. Ramesh, G.P.C. Rao, K. Seshaiah, Removal of copper and cadmium from the aqueous solutions by activated carbon derived from *Ceiba pentandra* hulls, J. Hazard. Mater. B129 (2006) 123–129.
[5] S.E. Bailey, T.J. Olin, R.M. Bricka, D.D. Adrian, A review of potentially low-cost sorbents for heavy metals, Water Res. 33 (1999) 2469–2479.
[6] K.S. Low, C.K. Lee, S.C. Liew, Sorption of cadmium and lead from aqueous solutions by spent grain, Process Biochem. 36 (2000) 59–64.
[7] R.A. Shawabkeh, D.A. Rockstraw, R.K. Bhada, Copper and strontium adsorption by a novel carbon material manufactured from pecan shells, Carbon 40 (2002) 781–786.
[8] S.A. Dastgheib, D.A. Rockstraw, Pecan shell activated carbon: synthesis, characterization, and application for the removal of copper from aqueous solution, Carbon 39 (2001) 1849–1855.
[9] G. Cimino, A. Passerini, G. Toscano, Removal of toxic cations and Cr(VI) from aqueous solution by hazelnut shell, Water Res. 34 (2000) 2955–2962.
[10] E. Demirbas, Adsorption of cobalt(II) from aqueous solution onto activated carbon prepared from hazelnut shells, Adsorption Sci. Technol. 21 (2003) 951–963.
[11] M. Kobya, Adsorption kinetic and equilibrium studies of Cr(VI) by hazelnut shell activated carbons, Adsorption Sci. Technol. 22 (2004) 51–64.
[12] E. Sayan, Ultrasound-assisted preparation of activated carbon from alkaline impregnated hazelnut shell: an optimization study on removal of Cu^{2+} from aqueous solution, Chem. Eng. J. 115 (2006) 213–218.
[13] K. Periasamy, C. Namasivayam, Removal of Cu(II) by adsorption onto peanut hull carbon from water and copper plating industry wastewater, Chemosphere 32 (1996) 769–789.
[14] C. Namasivayam, K. Kadirvelu, Agricultural solid wastes for the removal of heavy metals: Adsorption of Cu(II) by coirpith carbon, Chemosphere 34 (1997) 377–399.
[15] D. Kavitha, C. Namasivayam, Experimental and kinetic studies on methylene blue adsorption by coir pith carbon, Bioresour. Technol. 98 (2007) 14–21.
[16] M.L. Martinez, M.M. Torres, C.A. Guzman, D.M. Maestri, Preparation and characteristics of activated carbon from olive stones and walnut shells, Ind. Crops Prod. 23 (2006) 23–28.
[17] M.A. Ferro Garcia, J. Rivera Ultrilla, J. Rodriguez Gordillo, I. Bautista Toledo, Adsorption of zinc, cadmium, and copper on activated carbons obtained from agricultural by-products, Carbon 26 (1988) 363–373.
[18] E. Demirbas, M. Kobya, A.E.S. Konukman, Error analysis of equilibrium studies for the almond shell activated carbon adsorption of Cr(VI) from aqueous solutions, J. Hazard. Mater. 154 (2008) 787–794.
[19] A.A. Amina, S.G. Badie, A.F. Nady, Removal of methylene blue by carbons derived from peach stones by H_3PO_4 activation: batch and column studies, Dyes Pigments 76 (2008) 282–289.
[20] N. Spahis, A. Addoun, H. Mahmoudi, N. Ghaffour, Purification of water by activated carbon prepared from olive stones, Desalination 222 (2008) 519–527.
[21] M.H. Kalavathy, T. Karthikeyan, S. Rajgopal, L.R. Miranda, Kinetic and isotherm studies of Cu(II) adsorption onto H_3PO_4-activated rubber wood sawdust, J. Colloid Interface Sci. 292 (2005) 354–362.
[22] A. Demirbas, Kinetics for non-isothermal flash pyrolysis of hazelnut shell, Bioresour. Technol. 66 (1998) 247–252.
[23] S. Lagergren, About the theory of so called adsorption of soluble substances, Ksver Veterskapsakad Handl. 24 (1898) 1–6.
[24] Y.S. Ho, G. McKay, Pseudo-second order model for sorption processes, Process Biochem. 34 (1999) 451–465.
[25] S.H. Chien, W.R. Clayton, Application of Elovich equation to the kinetics of phosphate release and sorption in soils, Soil Sci. Soc. Am. J. 44 (1980) 265–268.
[26] K. Urano, H. Tachikawa, Process development for removal and recovery of phosphorus from wastewater by a new adsorbent. II. Adsorption rates and breakthrough curves, Ind. Eng. Chem. Res. 30 (1991) 1897–1899.
[27] X.C. Chen, Y.P. Wang, Q. Lin, J.Y. Shi, W.X. Wu, Y.X. Chen, Biosorption of copper(II) and zinc(II) from aqueous solution by *Pseudomonas putida* CZ1, Colloids Surf. B: Biointerfaces 46 (2005) 101–107.
[28] Y.S. Ho, C.C. Chiang, Y.C. Hsu, Sorption kinetics for dye removal from aqueous solution using activated clay, Sep. Sci. Technol. 36 (2001) 2473–2488.
[29] K.K. Wong, C.K. Lee, K.S. Low, M.J. Haron, Removal of Cu and Pb by tartaric acid modified rice husk from aqueous solutions, Chemosphere 50 (2003) 23–28.
[30] D. Chazopoulos, A. Varma, R.L. Irvine, Activated carbon adsorption and desorption of toluene in the aqueous phase, AIChE J. 39 (1993) 2027–2041.
[31] M.A.M. Khraisheh, Y.S. Al-Degs, S.J. Allen, M.N. Ahmad, Elucidation of controlling steps of reactive dye adsorption on activated carbon, Ind. Eng. Chem. Res. 41 (2002) 1651–1657.
[32] X.S. Wang, Y. Qin, Equilibrium sorption isotherms of Cu^{2+} on rice bran, Process Biochem. 40 (2005) 677–680.
[33] D. Brady, J.R. Duncan, Bioaccumulation of metal cations by *Saccharomyes cerevisiae*, Appl. Microbiol. Biotechnol. 41 (1994) 149–154.
[34] A. Shukla, Y.H. Zhang, P. Dubey, J.L. Margrave, S.S. Shukla, The role of sawdust in the removal of unwanted materials fromwater, J. Hazard. Mater. B95 (2002) 137–152.
[35] I. Langmuir, The adsorption of gases on plane surface of glass, mica, and platinum, J. Am. Chem. Soc. 40 (1918) 1361–1403.
[36] H. Freundlich, Adsorption in solution, Z. Phys. Chem. 57 (1906) 384–410.

[37] M.J. Tempkin, V. Pyzhev, Kinetics of ammonia synthesis on promoted iron catalysts, Acta Physiochim. URSS 12 (1940) 217–222.
[38] A.K. Bhattacharya, T.K. Naiya, S.N. Mandal, S.K. Das, Adsorption, kinetics and equilibrium studies on removal of Cr(VI) from aqueous solutions using different low-cost adsorbents, Chem. Eng. J. 137 (2008) 529–541.
[39] G. McKay, M.S. Otterburn, A.J. Aga, Fuller's earth and fired clay as adsorbents for dyestuffs, Water Air Soil Pollut. 24 (1985) 307–322.
[40] M. Alkan, B. Kalay, M. Dogan, O. Demirbas, Removal of copper ions from aqueous solutions by kaolinite and batch design, J. Hazard. Mater. 153 (2008) 867–876.
[41] W. Chung-Hsin, Studies of the equilibrium and thermodynamics of the adsorption of Cu^{2+} onto as-produced and modified carbon nanotubes, J. Colloid Interface Sci. 311 (2007) 338–346.